

## A Rothe-immersed Interface Method for an Elliptic-parabolic Interface Problem

Ivan Georgiev

**Abstract.** This paper deals with the construction and theoretical analysis of a Rothe's FE-IIM for a model elliptic-parabolic problem. Numerical experiments are also discussed.

**Key words:** elliptic-parabolic problems, interface problems, FEM.

### INTRODUCTION

This paper concerns what we term a parabolic-elliptic interface problem. Two – dimensional problems are investigated in many papers [1-4]. They arise in the study of two-dimensional eddy currents [2], in the quasistationary two-dimensional magnetic fields [1], surface measurements [3], etc. In the present paper we shall concentrate on the following simplified model from the biochemical reactor theory [ 4]:

$$-\mu_E \frac{\partial^2 c}{\partial x^2} + f(x)c = g_1(x, y) \text{ in } \Omega_E = (0, \xi) \times (0, 1), \quad (1)$$

$$v \frac{\partial c}{\partial y} - \mu_P \frac{\partial^2 c}{\partial x^2} = g_2(x, y) \text{ in } \Omega_P = (\xi, 1) \times (0, 1), \quad (2)$$

with boundary conditions

$$c(x, 0) = c_0(x) \quad , \quad \xi < x < 1, \quad (3)$$

$$c(0, y) = g_3(y); c(1, y) = g_4(y); \quad , \quad 0 < y < 1, \quad (4)$$

and interface conditions

$$[c]_{x=\xi} = c(\xi^+, y) - c(\xi^-, y) = 0, \quad (5)$$

$$\left[ \mu \frac{\partial c}{\partial x} \right]_{x=\xi} = \mu_E \frac{\partial c}{\partial x}(\xi^+, y) - \mu_P \frac{\partial c}{\partial x}(\xi^-, y) = 0. \quad (6)$$

In (1), (2),  $\mu_E, \mu_P$ , are given positive constants.

The problem is elliptic in  $\Omega_E$  and parabolic in  $\Omega_P$ .

Let introduce the Sobolev space  $H^1(0,1)$  and the bilinear form:

$$a(c, \varphi) = \int_0^\xi \frac{\partial c}{\partial x} \frac{d\varphi}{dx} dx + \frac{\mu_P}{\mu_E} \int_\xi^1 \frac{\partial c}{\partial x} \frac{d\varphi}{dx} dx, \quad \varphi \in H^1(0,1). \quad (7)$$

Let denote by  $(\cdot, \cdot), (\cdot, \cdot)_E, (\cdot, \cdot)_P$  the inner products respectively in  $L^2(0,1), L^2(0, \xi), L^2(\xi, 1)$ .

The equation (1) and (2) could be written in the equivalent form:

$$(v \frac{\partial c}{\partial y}, \varphi) + \mu_E a(c, \varphi) + (f(x)c, \varphi) = 0 \quad \forall \varphi \in H^1(0,1). \quad (8)$$

Using energy methods in [6], one can prove that, if  $f \in L^2(\Omega_E)$ ,  $g_1, g_2 \in L^2(\Omega_E \cup \Omega_p)$  then the problem (1)-(6) has unique solution  $c \in L^2(0,1; H^1(0,1))$  and  $\partial c / \partial x \in L^2(0,1; H^{-1}(0,1))$ .

In Rothe's method [6] we apply an  $y$ -semidiscretization to approximate the parabolic part (1) of the problem by a finite sequence of elliptic interface boundary value problems. In Section 2 on each  $y$  - level we solve the corresponding elliptic problem by the FE-IIM, see [5]. Numerical experiments are discussed in the last section.

### Rothe's FE-IIM

Let us divide the interval  $[0,1]$  by an equidistant mesh of step size  $\tau = 1/M$ . Let  $z_m(x)$  denote the computed approximation of  $c(x, y_m)$  at each  $y$ - level  $y_m = m\tau$ ,  $m = 0, 1, \dots, M$ . These approximations are defined iteratively by

$$-\mu_E z_m''(x) + f(x)z_m = g_1(x, y_m), \quad x \in (0, \xi), \quad (9)$$

$$v \frac{z_m(x) - z_{m-1}(x)}{\tau} - \mu_p z_m''(x) = g_2(x, y_m), \quad x \in (\xi, 1) \quad (10)$$

$$z_0(x) = c_0(x), \quad x \in (\xi, 1). \quad (11)$$

with boundary conditions

$$c_m(0, y_m) = g_3(y_m), \quad c_m(1, y_m) = g_4(y_m), \quad (12)$$

and interface conditions

$$[z_m]_{x=\xi} = c(\xi^+, y_m) - c(\xi^-, y_m) = 0, \quad (13)$$

$$[\mu_E']_{x=\xi} = 0. \quad (14)$$

This approximate solution can be extended from its values at the grid points  $y_j$  to all  $y \in [0,1]$  by setting

$$c^\tau(x, y) = z_{m-1}(x) + \frac{y - y_{m-1}}{\tau} [z_m(x) - z_{m-1}(x)] \quad \text{on} \quad [y_{j-1}, y_j] \quad \text{for} \quad j = 1, \dots, M.$$

We rewrite the equations (9) and (10) in the form

$$(\beta_m(x) z_m'' + q_m(x) z_m = r_m(x), \quad (15)$$

$$\beta_m(x) = \begin{cases} -\mu_E, & \\ -\mu_p, & \end{cases} \quad q_m(x) = \begin{cases} f(x), & \\ v/\tau, & \end{cases} \quad r_m(x) = \begin{cases} g_1(x, y_m), & \\ g_2(x, y_m) + \frac{v}{\tau} z_{m-1}(x). & \end{cases}$$

Now we are in position to apply to the boundary value problem (15), (12), (13), (14) the FE-IIM proposed in [5]. We use an uniform grid  $x_i = ih$ ,  $i = 0, \dots, N$  with  $x_0 = 0$ ,  $x_N = 1$  and  $h = 1/N$ . The standard linear basis function satisfies:

$$\phi_i = \begin{cases} 1, & \text{if } i = k \\ 0, & \text{otherwise.} \end{cases}$$

The numerical solution  $z_m^h(x) = \sum_{i=0}^N c_i \phi_i(x)$ , (with unknowns  $c_i$ ) is a combination of the special basis, see [5]. If  $x_j < \xi < x_{j+1}$ , then  $\phi_j$  and  $\phi_{j+1}$  need to be changed to satisfy the second jump conditions (13), (14) which implies :

$$\phi_j(x) = \begin{cases} 0, & 0 \leq x < x_{j-1} \\ \frac{x - x_{j-1}}{h}, & x_{j-1} \leq x < x_j \\ \frac{x_j - x}{k}, & x_j \leq x < \xi \\ \frac{\rho(x_{j+1} - x)}{k}, & \xi \leq x < x_{j+1} \\ 0, & x_{j+1} \leq x \leq 1 \end{cases} \quad \phi_{j+1}(x) = \begin{cases} 0, & 0 \leq x < x_j \\ \frac{x - x_j}{k}, & x_j \leq x < \xi \\ \frac{\rho(x - x_{j+1})}{k} + 1, & \xi \leq x < x_{j+1} \\ \frac{x_{j+2} - x}{h}, & x_{j+1} \leq x < x_{j+2} \\ 0, & x_{j+2} \leq x \leq 1 \end{cases}$$

where: 
$$\rho = \frac{v\mu_E}{\mu_p}, \quad k = h - \frac{v\mu_E - \mu_p}{v\mu_E}(\xi - x_j).$$

Combining results from [5,6] one can prove the following theorem.

**Theorem 1.** Suppose that the assumptions for the weak form (7), (8) of problem (1)-(4) are fulfilled. Then for the Rothe's FE-IIM solution  $c_h^\tau$  the estimate holds

$$\|c_h^\tau - c\| \leq C(\tau + h^2), \tag{16}$$

where the constant  $C$  is independent of  $\tau, h$ .

### NUMERICAL EXPERIMENTS

For the numerical experiments we consider the following test problem:

$$-\mu_E \frac{\partial^2 c}{\partial x^2} + fc = g_1(x, y), \quad \text{in } \Omega_E = (0, \frac{\pi}{6}) \times (0, 1),$$

$$\frac{\partial c}{\partial y} - \mu_p \frac{\partial^2 c}{\partial x^2} = g_2(x, y), \quad \text{in } \Omega_p = (\frac{\pi}{6}, 1) \times (0, 1),$$

where we chose  $\mu_E = 1, \mu_p = \sqrt{3}, f = 1, g_1(x, y) = g_2(x, y) = 0$ , and an exact solution

$$c(x, y) = \begin{cases} \cos(\pi/6) \exp(\pi/6 - \sqrt{3}y - x), & 0 \leq x \leq \pi/6, 0 \leq y \leq 1 \\ \cos(x) \exp(\sqrt{3}y) & 0 \leq x \leq \pi/6, 0 \leq y \leq 1 \end{cases}. \tag{17}$$

The boundary conditions  $g_3(y), g_4(y)$ , and  $c_0(x)$  are founded from the exact solution (17).

We examine two types of basis functions. First case: The interface  $\xi$  is a grid point, i.e. we divide  $(0, \xi)$  in  $N_1$  regular subintervals with mesh size  $h_1 = \xi / N_1$  and  $(\xi, 1)$  in  $N_2$ .

The numerical experiments are presented in Table 1, where

$$\|er\|_\infty = \max(|c(x_i, y_i) - c_h^\tau(i, j)|) \text{ is the error in maximum norm, ratio is } \text{ratio} = \frac{\|er_{N_1, N_2}^M\|_\infty}{\|er_{2N_1, 2N_2}^{4M}\|_\infty},$$

$m$  is the rate of convergence, calculated by the formula  $m = \log_2(\text{ratio})$ .

Ratio near 4 corresponds to second order of accuracy of the method in space direction  $x$ .

In Figure 1 the numerical solution for  $N_1 = 40, N_2 = 40, M = 640$  is presented. Also, in Figure2 the error in maximum norm is depicted.

Second case: The interface  $\xi$  is not a grid point i.e. we divide  $(0, 1)$   $N$  regular intervals. The numerical experiments are given in Table 2. The results show again the second order of the method in depends of  $x$  variable. The error is bigger on the interface  $x = \pi/6, y \in (0, 1)$ . In figure 3 the error in maximum norm if the interface  $x = \xi$  is not a grid point, is presented.

Table1. Mesh refinement analysis for the case, when the interface is a grid point.

N1	N2	M	$\ er\ _{\infty}$	ratio	m
5	5	10	0.0036	-	-
10	10	40	9.8000e-004	3.6735	1.8771
20	20	160	2.5338e-004	3.8677	1.9515
40	40	640	6.3967e-005	3.9611	1.9859
80	80	2560	1.6030e-005	3.9905	1.9966

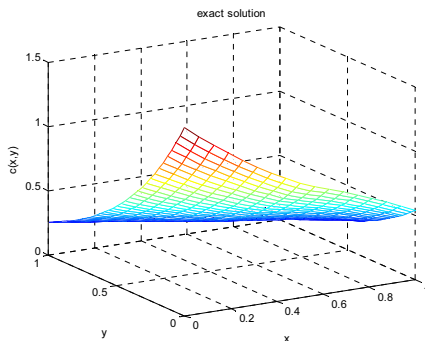


Figure1. The exact solution

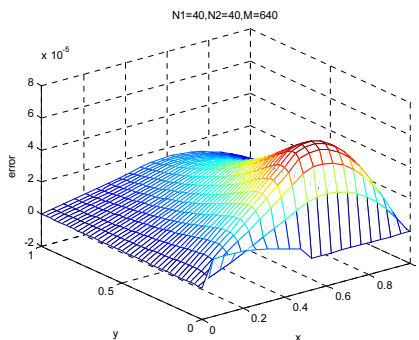


Figure 2. The error of the numerical solution in maximum norm, when the interface is a grid point.

Table 2. Mesh refinement analysis for the case, when the interface is not a grid point.

N	M	$\ c\ _{\infty}$	ratio	m
20	1000	0.0452	-	-
40	1000	0.0098	4.6122	2.2055
80	1000	0.0022	4.4545	2.1553
160	1000	5.3602e-004	4.1043	2.0371
320	1000	1.6400e-004	3.2684	1.7086

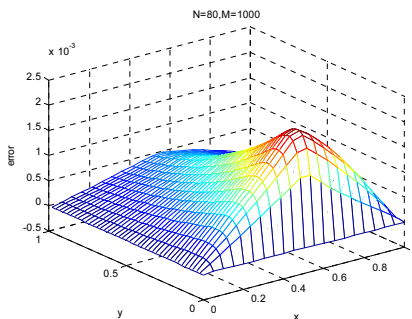


Figure3. The error of the numerical solution in maximum norm, when the interface is not a grid point.

### CONCLUSION

The problem treated here is a simplification in on-space dimension of 2D-curve and 3D-surface interface problems occurring in physics and engineering. We have employed the Rothe method in combination with the FE-IIM. The experiment show that this method is very accurate for 1D problems and very promising for 2D. Progress has been made in the 2D-case , but further theoretical work is needed.

### Acknowledgements

This work was supported in part by National Science Fund of Bulgaria under contract HS-MI-106/2005 and partially by the project 2008-FPNO-05 of RU.

### REFERENCE

- [1] Al-Droubi A., M. Renardy Energy methods for a parabolic-hyperbolic interface problem arising in electromagnetism. *J. Appl. Math. Phys.* , 1988, 39, 931—936.
- [2] Al-Droubi A. A two-dimensional eddy current problem. Ph. D. thesis, Carnegie-Mellon University, Pittsburgh, 1987.
- [3] Fruhauf F., B. Gebaner, O. Scherzer. Detecting interfaces in parabolic-elliptic problem from surface measurements. *SIAM J. Numer. Anal.*, 2008, 45/2, 810-836.
- [4] Henry J. Optimization of fermentation reactor with non-moving layer. *Num. Meth. in Appl. Math.*, Science, Siberian Branch, 1982, 163-173.
- [5] Li Z. The immersed interface method using a finite element formulation. *Appl. Num. Math.*, 1998, 27/3, 253-267.
- [6] Rektorys K. The method of discretization in time. SNTL, Prague, 1982.

### За контакти:

Иван Радославов Георгиев , Катедра “Числени методи и статистика”, Русенски университет “Ангел Кънчев”, тел.: 082-888 725, e-mail: [irgeorgiev@ru.acad.bg](mailto:irgeorgiev@ru.acad.bg)

**Докладът е рецензиран.**